Direct Measurements of A_b and A_c using Vertex/Kaon Charge Tags at SLD[*]

Koya Abe,[25] Kenji Abe,[15] T. Abe,[22] I. Adam,[22] H. Akimoto,[22] D. Aston,[22]
K.G. Baird,[11] C. Baltay,[31] H.R. Band,[30] T.L. Barklow,[22] J.M. Bauer,[12]
G. Bellodi,[17] R. Berger,[22] G. Blaylock,[11] J.R. Bogart,[22] G.R. Bower,[22] J.E. Brau,[16]
M. Breidenbach,[22] W.M. Bugg,[24] D. Burke,[22] T.H. Burnett,[29] P.N. Burrows,[19]
A. Calcaterra,[8] R. Cassell,[22] A. Chou,[22] H.O. Cohn,[24] J.A. Coller,[4]
M.R. Convery,[22] V. Cook,[29] R.F. Cowan,[13] G. Crawford,[22] C.J.S. Damerell,[21]
M. Daoudi,[22] S. Dasu,[30] N. de Groot,[2] R. de Sangro,[8] D.N. Dong,[13] M. Doser,[22]
R. Dubois,[22] I. Erofeeva,[14] V. Eschenburg,[12] E. Etzion,[30] S. Fahey,[5] D. Falciai,[8]
J.P. Fernandez,[27] K. Flood,[11] R. Frey,[16] E.L. Hart,[24] K. Hasuko,[25]
S.S. Hertzbach,[11] M.E. Huffer,[22] X. Huynh,[22] M. Iwasaki,[16] D.J. Jackson,[21]
P. Jacques,[20] J.A. Jaros,[22] Z.Y. Jiang,[22] A.S. Johnson,[22] J.R. Johnson,[30]
R. Kajikawa,[15] M. Kalelkar,[20] H.J. Kang,[20] R.R. Kofler,[11] R.S. Kroeger,[12]
M. Langston,[16] D.W.G. Leith,[22] V. Lia,[13] C. Lin,[11] G. Mancinelli,[20] S. Manly,[31]
G. Mantovani,[18] T.W. Markiewicz,[22] T. Maruyama,[22] A.K. McKemey,[3]
R. Messner,[22] K.C. Moffeit,[22] T.B. Moore,[31] M. Morii,[22] D. Muller,[22] V. Murzin,[14]
S. Narita,[25] U. Nauenberg,[5] H. Neal,[31] G. Nesom,[17] N. Oishi,[15] D. Onoprienko,[24]
L.S. Osborne,[13] R.S. Panvini,[28] C.H. Park,[23] I. Peruzzi,[8] M. Piccolo,[8]
L. Piemontese,[7] R.J. Plano,[20] R. Prepost,[30] C.Y. Prescott,[22] B.N. Ratcliff,[22]
J. Reidy,[12] P.L. Reinertsen,[27] L.S. Rochester,[22] P.C. Rowson,[22] J.J. Russell,[22]
O.H. Saxton,[22] T. Schalk,[27] B.A. Schumm,[27] J. Schwiening,[22] V.V. Serbo,[22]
G. Shapiro,[10] N.B. Sinev,[16] J.A. Snyder,[31] H. Staengle,[6] A. Stahl,[22] P. Stamer,[20]
H. Steiner,[10] D. Su,[22] F. Suekane,[25] A. Sugiyama,[15] A. Suzuki,[15] M. Swartz,[9]
F.E. Taylor,[13] J. Thom,[22] E. Torrence,[13] T. Usher,[22] J. Va'vra,[22] R. Verdier,[13]
D.L. Wagner,[5] A.P. Waite,[22] S. Walston,[16] A.W. Weidemann,[24] E.R. Weiss,[29]
J.S. Whitaker,[4] S.H. Williams,[22] S. Willocq,[11] R.J. Wilson,[6] W.J. Wisniewski,[22]
J.L. Wittlin,[11] M. Woods,[22] T.R. Wright,[30] R.K. Yamamoto,[13] J. Yashima,[25]
S.J. Yellin,[26] C.C. Young,[22] H. Yuta.[1]

[1] *Aomori University, Aomori, 030 Japan,*
[2] *University of Bristol, Bristol, United Kingdom,*
[3] *Brunel University, Uxbridge, Middlesex, UB8 3PH United Kingdom,*
[4] *Boston University, Boston, Massachusetts 02215,*
[5] *University of Colorado, Boulder, Colorado 80309,*
[6] *Colorado State University, Ft. Collins, Colorado 80523,*
[7] *INFN Sezione di Ferrara and Universita di Ferrara, I-44100 Ferrara, Italy,*

$^{(8)}$*INFN Laboratori Nazionali di Frascati, I-00044 Frascati, Italy,*
$^{(9)}$*Johns Hopkins University, Baltimore, Maryland 21218-2686,*
$^{(10)}$*Lawrence Berkeley Laboratory, University of California, Berkeley, California 94720,*
$^{(11)}$*University of Massachusetts, Amherst, Massachusetts 01003,*
$^{(12)}$*University of Mississippi, University, Mississippi 38677,*
$^{(13)}$*Massachusetts Institute of Technology, Cambridge, Massachusetts 02139,*
$^{(14)}$*Institute of Nuclear Physics, Moscow State University, 119899 Moscow, Russia,*
$^{(15)}$*Nagoya University, Chikusa-ku, Nagoya, 464 Japan,*
$^{(16)}$*University of Oregon, Eugene, Oregon 97403,*
$^{(17)}$*Oxford University, Oxford, OX1 3RH, United Kingdom,*
$^{(18)}$*INFN Sezione di Perugia and Universita di Perugia, I-06100 Perugia, Italy,*
$^{(19)}$*Queen Mary, University of London, London, E1 4NS United Kingdom,*
$^{(20)}$*Rutgers University, Piscataway, New Jersey 08855,*
$^{(21)}$*Rutherford Appleton Laboratory, Chilton, Didcot, Oxon OX11 0QX United Kingdom,*
$^{(22)}$*Stanford Linear Accelerator Center, Stanford University, Stanford, California 94309,*
$^{(23)}$*Soongsil University, Seoul, Korea 156-743,*
$^{(24)}$*University of Tennessee, Knoxville, Tennessee 37996,*
$^{(25)}$*Tohoku University, Sendai, 980 Japan,*
$^{(26)}$*University of California at Santa Barbara, Santa Barbara, California 93106,*
$^{(27)}$*University of California at Santa Cruz, Santa Cruz, California 95064,*
$^{(28)}$*Vanderbilt University, Nashville,Tennessee 37235,*
$^{(29)}$*University of Washington, Seattle, Washington 98105,*
$^{(30)}$*University of Wisconsin, Madison,Wisconsin 53706,*
$^{(31)}$*Yale University, New Haven, Connecticut 06511.*

Abstract

Exploiting the manipulation of the SLC electron-beam polarization, we present precise direct measurements of the parity violation parameters A_c and A_b in the Z boson–c quark and Z boson–b quark coupling. Quark/antiquark discrimination is accomplished via a unique algorithm that takes advantage of the precise SLD CCD vertex detector, employing the net charge of displaced vertices as well as the charge of kaons that emanate from those vertices. From the 1996-98 sample of 400,000 Z decays, produced with an average beam polarization of 73.4%, we find $A_c = 0.673 \pm 0.029(\text{stat.}) \pm 0.023(\text{syst.})$ and $A_b = 0.919 \pm 0.018(\text{stat.}) \pm 0.017(\text{syst.})$.

Submitted to Physical Review Letters

Measurements of fermion production asymmetries at the Z^0 pole determine the extent of parity violation in the $Zf\bar{f}$ coupling. At Born level, the differential cross section for the process $e^+e^- \to Z^0 \to f\bar{f}$ can be expressed as a function of the polar angle θ of the fermion relative to the electron beam direction,

$$\frac{d\sigma_f}{d\cos\theta} \propto (1 - A_e P_e)(1 + \cos^2\theta) + 2A_f(A_e - P_e)\cos\theta, \tag{1}$$

where P_e is the longitudinal polarization of the electron beam ($P_e > 0$ for predominantly right-handed polarized beam). The parameter $A_f = 2v_f a_f/(v_f^2 + a_f^2)$, where v_f (a_f) is the vector (axial vector) coupling of the fermion f to the Z^0 boson, expresses the extent of parity violation in the $Zf\bar{f}$ coupling.

From the conventional forward-backward asymmetries formed with an unpolarized electron beam ($P_e = 0$), such as that used by the CERN Large Electron-Positron Collider (LEP) experiments, only the product $A_e A_f$ of parity-violation parameters can be measured [1]. With a longitudinally polarized electron beam, however, it is possible to measure A_f independently of A_e by fitting simultaneously to the differential cross sections of Eq. (1) formed separately for predominantly left- and right-handed beam. The resulting direct measurement of A_f is largely independent of propagator effects that modify the effective weak mixing angle, and thus is complementary to other electroweak asymmetry measurements performed at the Z^0 pole.

In this Letter, we present measurements of A_c and A_b based on the use of the invariant mass of displaced vertices to select $Z \to c\bar{c}$ and $Z \to b\bar{b}$ events. The charge of the underlying quark is determined via a unique algorithm that exploits the net charge of the displaced vertices, as well as the charge of tracks emanating from the vertices that are identified as kaons.

The operation of the SLC with a polarized electron beam has been described elsewhere [2]. During the 1996-98 run, the SLC Large Detector (SLD) [3, 4] recorded an integrated luminosity of 14.0 pb^{-1}, at a mean center-of-mass energy of 91.24 GeV, and with a luminosity-weighted mean electron-beam polarization of $|P_e| = 0.734 \pm 0.004$ [5].

The SLD measures charged particle tracks with the Central Drift Chamber (CDC), which is immersed in a uniform axial magnetic field of 0.6T. The VXD3 vertex detector provides an accurate measure of particle trajectories close to the beam axis. For the 1996-98 data, the combined $r\phi$ (rz) impact parameter resolution of the CDC and VXD3 is 7.8 (9.7) μm

3

at high momentum, and 34 (34) μm at $p_\perp\sqrt{\sin\theta} = 1$ GeV/c, where $p_\perp$ is the momentum transverse to the beam direction, and r (z) is the coordinate perpendicular (parallel) to the beam axis. The combined momentum resolution in the plane perpendicular to the beam axis is $\delta p_\perp/p_\perp = \sqrt{(.01)^2 + (.0026\ p_\perp/GeV/c)^2}$. A Cerenkov Ring-Imaging Detector (CRID) [6], using a combination of liquid and gaseous radiators, allows efficient $K - \pi$ separation in the range $0.3\ GeV/c < p_K < 30 GeV/c$ for tracks with $|\cos\theta| < 0.68$. The thrust axis is reconstructed using the Liquid Argon Calorimeter, which covers the angular range $|\cos\theta| < 0.98$. We employ a Monte Carlo (MC) simulation of the production and detection processes that makes use of the JETSET 7.4 event generator [7], the QQ [8] package for B hadron decay specially tuned to match the CLEO inclusive D production distributions [9] and the ARGUS particle production distributions [10], and the GEANT 3.21 framework [11] for the simulation of the SLD detector.

Events are classified as hadronic Z^0 decays if they: (1) contain at least seven well-measured tracks (as described in Ref. [3]); (2) exhibit a visible charged energy of at least 18 GeV; (3) have a thrust axis polar angle satisfying $|\cos\theta_{thrust}| < 0.7$; and (4) have a thrust magnitude greater than 0.8 (to suppress events with both heavy hadrons in the same hemisphere). Vertex identification is done using a topological algorithm [12], enhanced via the application of a neural-network selection based on the flight distance and angle of the reconstructed vertex[13]. According to the MC, secondary vertices are found in 72.7% of bottom-quark, 28.2% of charm-quark, and 0.41% of light-quark event hemispheres.

Due to the cascade nature of B decays, tracks from the decay may not all originate from the same space point. An independent neural network, exploiting the location of the point of closest approach of the track to the line connecting the primary and secondary vertices [13], is used to attach tracks with two or more VXD hits that are not already included in the secondary vertex. 'VXD-only' tracks with three or more VXD hits, but no CDC segment, are also considered for attachment; if attached, the fit vertex location is used as an additional space point to improve the charge determination.

A final neural network, making use of the p_T-corrected vertex mass (M_{VTX}) [14], the total momentum of the vertexed tracks (P_{VTX}), the flight distance from the IP to the vertex, and the number of tracks in the vertex [13], is used to discriminate between bottom and charm events. The output y_{hem} of this neural net is shown in Figure 1.

The analysis makes use of two mutually exclusive tags. The L-tag, optimized to select c

FIG. 1: Output distribution from the flavor-selection neural network; the separate bottom, charm, and uds contributions are derived from MC simulation.
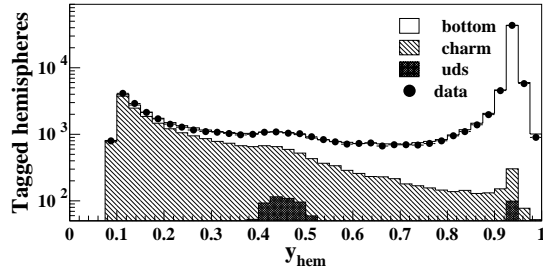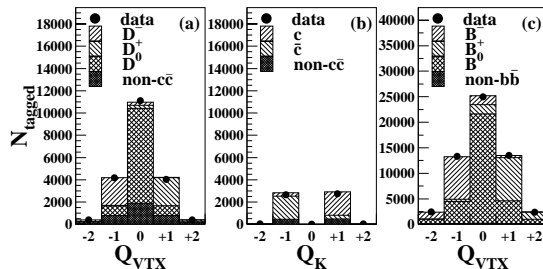

FIG. 2: Distributions of hemisphere charge: (a) Q_{vtx}, $y_{hem} < 0.4$; (b) Q_K, $y_{hem} < 0.4$ (the large $Q_K = 0$ contribution is suppressed); (c) Q_{vtx}, $y_{hem} > 0.85$, including VXD-only tracks. The D^+, D^-, D^0 and B^+, B^-, B^0 designations refer to all positive, negative, or neutral heavy flavor hadrons, including baryons, from the MC simulation.

hemispheres, requires $y_{hem} < 0.4$ and $P_{VTX} > 5$ GeV/c. The H-tag, optimized to select b requires $y_{hem} > 0.85$ and $M_{VTX} < 7$ GeV/c^2. From the MC simulation, we find that 84% (98%) of events with one (two) L-tagged hemisphere(s), and no H-tagged hemispheres, are $Z \to c\bar{c}$ decays, while 97% (100%) of events with one (two) H-tagged hemisphere(s) are $Z \to b\bar{b}$ decays.

Within tagged hemispheres, two quantities are used to discriminate quark from antiquark production: the net charge of all vertexed tracks (Q_{VTX}) and the net charge of all vertex tracks that are identified as kaons (Q_K). The presence of a quark is indicated by $Q_{VTX} > 0$ or $Q_K < 0$ for the L-tag, and $Q_{VTX} < 0$ for the H-tag; for this latter tag, the kaons do not make a significant additional contribution. If an L or H-tagged hemisphere cannot be assigned a nonzero charge using these methods, or if an L-tag has both Q_{VTX} and Q_K nonzero and in disagreement, it is treated as untagged. The resulting charge distributions are shown in Figure 2.

By comparing the tagging and sign-determination results between hemispheres in data

5

events, it is possible to determine most of the per-hemisphere tagging efficiencies ϵ_f^T and their correct-sign probabilities p_f^T for the tags $T = L, H$[13]. The fractions of single-H (XH), double-H (HH), mixed (HL), single-L (XL) and double-L (LL) tagged events are sensitive to the hemisphere tagging efficiencies; a maximum likelihood fit to these fractions is used to constrain the values of ϵ_c^L, ϵ_b^L, ϵ_c^H, and ϵ_b^H (Table I), assuming Standard Model (SM) values for the fraction R_b (R_c) of $b\bar{b}$ ($c\bar{c}$) events from e^+e^- annihilation at the Z^0 pole. The hemisphere correct-sign probabilities p_c^L, p_b^L, and p_b^H (Table I) are constrained by a similar fit to the fractions of oppositely-signed hemispheres in HH, HL, and LL events, using the previously determined tagging efficiencies as input.

In constraining the tagging efficiencies and correct-sign probabilities from the inter-hemisphere tagging and signing information, it is necessary to account for inter-hemisphere correlations that alter the nominal relationship between single-hemisphere and full-event tagging and charge signing performance. MC studies confirm that, for vertex-based tagging and signing, inter-hemisphere correlations are due primarily to correlation in the energy and angle of the hadrons containing the heavy quarks, and from events for which both heavy hadrons are produced in the same hemisphere. To account for these effects, we have used the MC simulation to explore the dependence of the tagging and signing parameters as a function of the number of heavy hadrons in the hemisphere, and of the polar angle and energy (after restricting to hemispheres with a single heavy hadron) of the heavy hadron. The effects of the inter-hemisphere correlations can then be accounted for by convolving these dependences with the distributions of the number, energy, and polar angle of heavy hadrons within and opposite to tagged hemispheres, as described in [13]. Ignoring these effects would incorrectly lower A_b and A_c by approximately 1.5% of their subsequent fit values.

The fit for the parameter A_c makes use of events with at least one L-tagged hemisphere and neither H-tagged, while the A_b fit uses events with at least one H tag. Events with two L or two H tags are discarded if the charges in the two hemispheres are in disagreement. For events with one H and one L tag, only the H tag is used to sign the thrust axis. From the MC simulation, we find that 84% (98%) of events with one L tag (two L tags) are $Z \to c\bar{c}$ events, while 97% (100%) of events with one H tag (two H tags) are $Z \to b\bar{b}$ events.

Unbinned maximum-likelihood fits are performed to the Born-level differential cross section:

$$\mathcal{L} \sim (1 - A_e P_e)(1 + \cos^2 \theta_{\hat{t}}) + 2(A_e - P_e)A_E \cos \theta_{\hat{t}} \tag{2}$$

TABLE I: Per-hemisphere efficiencies (requiring that hemispheres be tagged and have non-zero net charge) ϵ_v^T and correct-sign probabilities p_f^T. "Calib" refers to the values obtained from the calibration procedure described in [13], while the "MC" column shows the expectations from the simulation. p_c^H is not calibrated from the data and so is not shown.

	ϵ_{MC}	ϵ_{calib}	p_{MC}	p_{calib}
c, L-tag	0.121	0.115±0.002	0.932	0.918±0.010
b, L-tag	0.020	0.022±0.001	0.545	0.543±0.031
c, H-tag	0.005	0.006±0.002	—	—
b, H-tag	0.323	0.325±0.002	0.807	0.821±0.005

where $\theta_{\hat{t}}$ is the polar angle of the signed thrust axis, and the electron beam polarization is signed so that $P_e > 0$ for right-handed electrons. The fitted effective asymmetry A_E is given by the sum over the flavor composition of the sample:

$$A_E = \sum_f \Pi_f (2P_f - 1)(1 - C_f^{QCD})(A_f - \delta_f^{QED}) \tag{3}$$

where Π_f is the fraction of and P_f the correct-signing probability for the flavor f, calculated separately for single- and double-tagged events, making use of the values in Table I when possible. For the light flavor uds contribution, the simulated mistag rates are used for Π_{uds}, while P_{uds} is set to 0.5 ± 0.29 (uniform probability between 0 and 1). Mechanisms for developing a charm signal in the H-tagged sample tend to favor incorrect charge assignment [13], leading to the assumption $p_c^H = 0.25 \pm 0.14$. Because events at larger values of $|\cos \theta_{\hat{t}}|$ carry larger statistical weights in the fits, but poorer overall tagging qualities, the MC simulation is used to parameterize these values as a function of $\cos \theta_{\hat{t}}$. Failing to account for this effect would incorrectly lower the fitted values of A_c and A_b by 1-2%.

The corrections C_f^{QCD} for gluon radiation are evaluated as in [15]. The $\mathcal{O}(\alpha_S^2)$ corrections are evaluated in [1] as 4.5%(3.8%) for $c(b)$ events, using the calculation in [16] based on the parton thrust axis (we ignore the hadronization corrections of [1] since they are implicit in our signed thrust axis analyzing power). Additionally, the analysis procedure suppresses events with hard gluon radiation, and so these results are further scaled by factors s_f of 0.27±0.13(0.53±0.08) for C_c^{QCD} (C_b^{QCD}), as determined by the MC simulation.

The δ_f^{QED} terms correct the asymmetries for the effects of initial-state QED radiation and γ/Z interference, and are determined by ZFITTER [17] to be $\delta_c^{QED} = 0.0012$ and

$\delta_b^{QED} = -0.0021$.

From a sample of 9970 events, using the SM value $A_b = 0.935$ as input, we obtain $A_c = 0.6747 \pm 0.0290(\text{stat.})$, while from a sample of 25917 events, using the Standard Model value of $A_c = 0.667$ as input, we obtain $A_b = 0.9173 \pm 0.0184(\text{stat.})$.

We have explored a number of potential sources of systematic error; these are summarized in Table . For both A_c and A_b, the dominant systematic uncertainty arises from the limited statistics available for the calibration of the purity of the flavor-selected sample, and of the correct-sign tagging probability of the sample, resulting in a relative systematic uncertainty of $\pm 3.0\%$ ($\pm 1.5\%$) for A_c (A_b). By studying a sample enriched in uds quark production ($M_{hem} < 2$ GeV/c^2 and $P_{hem} < 4$ GeV/c), the fake-vertex efficiency ϵ_{uds} is constrained to be within 25% of its MC expectation, leading to uncertainties of $\pm 0.1\%$ ($\pm 0.0\%$) on A_c (A_b).

The procedure for calibrating the sample purity and correct-signing probabilities is subject to uncertainties in the correlation between the quark and antiquark energies, and in the fraction of events for which the quark and antiquark appear in the same hemisphere. Comparisons between data and MC of the correlation between the heavy hadron energies in c-quark and b-quark enriched samples constrain the c and b hadron energy correlations to be within 2.6% and 0.3% of their MC expectation (Table II), while comparisons of samples enhanced in three-jet production showed the same-hemisphere production rates to be within 1.1% and 0.7% of their MC expectations. The resulting overall uncertainty in A_c (A_b) due to tagging correlations is found to be 0.6% (0.3%).

The correction coefficients C_f^{theory} for hard gluon radiation ('QCD corrections') are subject to uncertainties in α_S, quark masses, and missing higher order terms, given by [1] as ± 0.0063 for both $f = c, b$. The determination of the scale factor s_f applied to account for the selection bias against events with hard gluon radiation is limited by Monte Carlo statistics to ± 0.13 (± 0.08) for s_c (s_b). The resulting overall uncertainty in the QCD correction is $\pm 0.6\%$ ($\pm 0.4\%$) for A_c (A_b).

Adding all sources of systematic error in quadrature, we find

$$A_c = 0.6747 \pm 0.0290(\text{stat.}) \pm 0.0233(\text{syst.}) \tag{4}$$

$$A_b = 0.9173 \pm 0.0184(\text{stat.}) \pm 0.0173(\text{syst.}). \tag{5}$$

Averaging these results (V) with complementary results for A_b using momentum-weighted track charge (Q) [18] and the charge of identified kaons from secondary vertices for data prior

to 1996 (K) [19], for A_c using fully-reconstructed charmed-meson decays (D) [20], and for A_c and A_b together using identified leptons (L) [21], we arrive at the overall SLD average of [22]

$$A_c = 0.6712 \pm 0.0224(\text{stat.}) \pm 0.0157(\text{syst.}) \tag{6}$$

$$A_b = 0.9170 \pm 0.0147(\text{stat.}) \pm 0.0145(\text{syst.}) \tag{7}$$

independent of the extent of parity violation in the coupling of the electron to the Z^0 boson, consistent with the Standard Model expectations of $A_c = 0.667$ and $A_b = 0.935$.

[1] D. Abbaneo et al. (LEP Electroweak Working Group), CERN-EP-2000-016 (2000).

[2] K. Abe et al., Phys. Rev. Lett. **78**, 2075 (1997).

[3] K. Abe et al., Phys. Rev. **D53**, 1023 (1996).

[4] K. Abe et al., Ann. Rev. Nucl. Part. Sci. **51**, 345 (2001).

[5] K. Abe et al., Phys. Rev. Lett. **84**, 5945 (2000), hep-ex/0004026.

[6] K. Abe et al., Nucl. Instrum. Meth. **A343**, 74 (1994).

[7] T. Sjostrand, Comput. Phys. Commun. **82**, 74 (1994).

[8] QQ - The CLEO Event Generator, http://www.lns.cornell.edu/public/CLEO/soft/QQ (unpublished).

[9] L. Gibbons et al., Phys. Rev. **D56**, 3783 (1997).

[10] H. Albrecht et al., Z. Phys. **C44**, 547 (1989).

[11] R. Brun, F. Bruyant, M. Maire, A. C. McPherson, and P. Zanarini, Tech. Rep. CERN-DD/EE/84-1 (1987).

[12] D. J. Jackson, Nucl. Instrum. Meth. **A388**, 247 (1997).

[13] T. Wright, SLAC-R-602 (2002).

[14] K. Abe et al., Phys. Rev. Lett. **80**, 660 (1998).

[15] D. Abbaneo et al. (LEP Heavy Flavor Working Group), Eur. Phys. J. **C4**, 185 (1998).

[16] S. Catani and M. H. Seymour, JHEP **07**, 023 (1999), hep-ph/9905424.

[17] D. Bardin et al., Comput. Phys. Commun. **133**, 229 (2001), hep-ph/9908433.

[18] K. Abe et al., Phys. Rev. Lett. **90**, 141804 (2003), hep-ex/0208044.

[19] K. Abe et al., Phys. Rev. Lett. **83**, 1902 (1999).

[20] K. Abe et al., Phys. Rev. **D63**, 032005 (2001), hep-ex/0009035.

[21] K. Abe et al., Phys. Rev. Lett. **83**, 3384 (1999).

[22] Statistical correlation coefficients ρ_{xy} were found to be $\rho_{VQ} = 0.32$, $\rho_{VL} = 0.15$, $\rho_{QL} = 0.22$, $\rho_{QK} = 0.08$, $\rho_{VK} = 0.00$, $\rho_{LK} = 0.04$ for the A_b measurement, and $\rho_{VD} = 0.12$, $\rho_{VL} = 0.05$, $\rho_{DL} = 0.07$ for the A_c measurement. Statistical and systematic correlations between the measurements were taken into account via the Best Linear Unbiased Estimator (BLUE) algorithm described by L. Lyons. , D. Gibaut, and P. Clifford, Nucl. Instr. Meth. **A270**, 110 (1988).

TABLE II: Relative systematic errors for the A_c and A_b measurements, in percent (%). "Remove" means to not apply the indicated correction to the Monte Carlo. A '+' ('-') sign indicates that A_f increases (decreases) if the true value of the parameter is larger than expected.

source	variation	$\delta A_c/A_c$	$\delta A_b/A_b$
Calibration statistics			
P_f	data statistics	2.96	1.41
Π_f	data statistics	0.68	0.63
EW parameters			
R_c	0.1723±0.0031	-0.18	+0.07
R_b	0.2163±0.0007	+0.25	-0.24
A_c	0.667±0.027	n/a	+0.04
A_b	0.935±0.021	-0.06	n/a
Detector modeling			
tracking efficiency	remove	-0.36	+0.34
tracking resolution	remove	-0.49	+0.04
CRID π mis-ID	data $\pm1\sigma$	-0.12	+0.00
QCD correction			
C_f^{theory}	±0.0063	+0.18	+0.35
s_f	±0.13, ±0.08	+0.59	+0.31
Backgrounds			
p_c^H	0.25±0.14	+0.83	-0.56
$g \rightarrow c\bar{c}$	2.96±0.38%	+0.22	+0.01
$g \rightarrow b\bar{b}$	0.254±0.051%	+0.06	-0.02
fake vertex ϵ_{uds}	±25%	+0.13	-0.01
fake vertex A_{uds}^{raw}	±0.6	-0.43	-0.09
Tagging correlations			
same-hemisphere $c\bar{c}$	2.82±1.13%	+0.33	-0.01
same-hemisphere $b\bar{b}$	2.45±0.74%	-0.04	+0.21
c energy correlation	1.4±2.6%	+0.48	-0.14
b energy correlation	1.4±0.3%	-0.07	+0.10
Other			
Beam polarization	±0.5%	-0.50	-0.50
MC statistics	±1σ	0.64	0.34
Total		3.48	1.89